

Fabrication methods based on wet etching process for the realization of silicon MEMS structures with new shapes

Prem Pal · Kazuo Sato

Received: 8 May 2009 / Accepted: 16 November 2009 / Published online: 21 February 2010
© Springer-Verlag 2010

Abstract In this paper, fabrication methods are developed in order to realize the silicon microelectromechanical systems components with new shapes in {100} Si wafers. Fabrication process utilizes wet etching with a single step of photolithography. The silicon etching is carried out in complementary metal oxide semiconductor process compatible pure and surfactant Triton-X-100 [$C_{14}H_{22}O(C_2H_4O)_n$, $n = 9-10$] added tetramethylammonium hydroxide (TMAH) solutions. The fabricated structures are divided in two categories: fixed and freestanding. The fixed structures are realized in single oxidized silicon wafers, while freestanding are formed in silicon nitride-based silicon on insulator (SOI) wafers. The SOI wafers are prepared by bonding the oxidized and the nitride deposited wafers, followed by thinning and chemical mechanical polishing processes. The etching results such as {100} and {110}Si etch rates, undercutting at rounded concave and sharp convex corners and etched surface morphologies are measured in both pure and Triton added TMAH solutions. Different concentrations of TMAH are used to optimize the etching conditions for desired etched profiles.

1 Introduction

There are two basic categories of etching processes: wet and dry etching. In micromachining technology, selection of the type of the etching depends upon the availability and requirement. In order to minimize the fabrication cost, which is the indispensable requirement of the industry, wet

anisotropic etching is preferred over dry one. The {111}Si planes in the wet anisotropic etchants etch very slowly while all other crystal planes etch rapidly. Consequently, only rectangle and squares can be generated in {100} silicon wafers with a high degree of precision. The undercutting at mask edges that are not aligned along $\langle 110 \rangle$ directions on {100} Si surface is a well known characteristic of the wet anisotropic etchants. Thus, silicon wet anisotropic etching offers both advantages and disadvantages due to crystallographic limitations. For instance, formation of square shaped cavities, V-grooves, and suspended structures by undercutting are some of the advantages of wet etching for the development of MEMS-based devices. On the other hand, for the fabrication of MEMS structures including sharp convex corners and curved edges such as proof mass for accelerometer, circular grooves, serpentine microfluidic channels, etc., wet etching is avoided owing to high undercutting at these types of corners and edges. However corner compensation method can be used to form the sharp convex corners, it cannot be used if structure includes rounded corners (or edges) (Pal et al. 2007a, b). In that case, only dry etching is the option as the etch rate is almost independent of crystallographic orientations (Bhardwaj et al. 1997). Moreover, CMOS process (or clean room) compatibility of etchant is also a serious concern especially when the etching step is attempted after the fabrication of CMOS circuitry. TMAH has gained wide popularity due to its clean room compatibility. In the last decade, different kinds of ionic and non-ionic surfactants are studied in TMAH to enhance the applications of wet etching in MEMS (Conway and Cunnane 2002; Jeon et al. 1996; Pal et al. 2007b, 2009; Resnik et al. 2005; Sarro et al. 2000; Sekimura 1999; Yang et al. 2005). The addition of a very small amount of surfactant in TMAH significantly reduces the etch rate of high index planes, resulting in a reduction of the undercutting at sharp convex,

P. Pal (✉) · K. Sato
Department of Micro-Nano Systems Engineering,
Nagoya University, Nagoya 464-8603, Japan
e-mail: prem@mech.nagoya-u.ac.jp

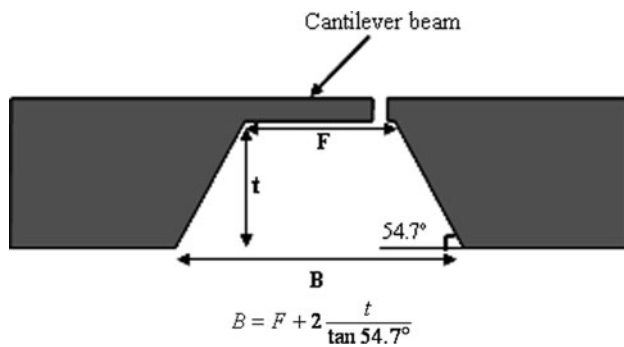


Fig. 1 Schematic view of wet bulk-micromachined suspended cantilever beams realized in {100} Si wafers using time-controlled backside etching

curved and non- $\langle 110 \rangle$ edges. Interestingly, these studies provide the choice to select the etchant according to the requirement of undercutting (e.g. high or low). Hence,

TMAH (with and without surfactant) can be exploited to develop new processes/techniques for the formation of new shapes MEMS components in/on silicon wafers (Pal and Sato 2009a, b; Yang et al. 2005).

In order to fabricate the freestanding silicon MEMS structures using wet bulk micromachining, the lithography as well as etching is performed on both sides of the wafer as shown in Fig. 1 (Abedinov et al. 2001; Wu et al. 1993). First the shape and thickness of the structures are defined at the frontside of the wafer by photolithography and etching steps. Thereafter, the wafer is patterned on the backside with respect to the frontside patterns using a front-to-back alignment technique (Pal et al. 2006). In this case, the size of the backside patterns depends upon the wafer thickness (Fig. 1) and therefore, same mask cannot be adopted for different thickness wafers. Moreover, the silicon wet etching requires very time controlled in order to have tight control over the thickness of the released structures.

Fig. 2 Fabrication steps for the realization of silicon MEMS structures on single silicon {100} wafer in one step lithography. (a) Thermally oxidized silicon wafers, (b) patterning of oxide by photolithography, (c) silicon anisotropic etching in 25 wt.% TMAH + Triton, (d) removal of oxide

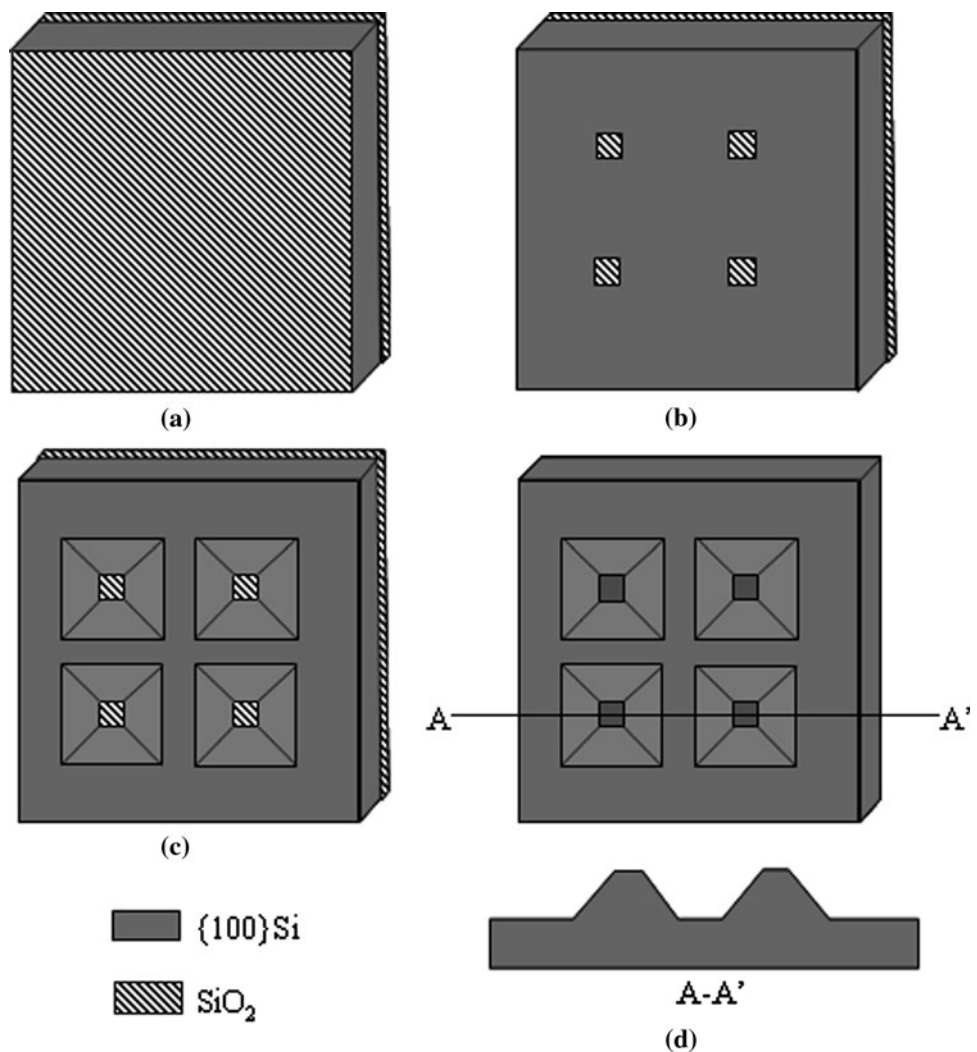
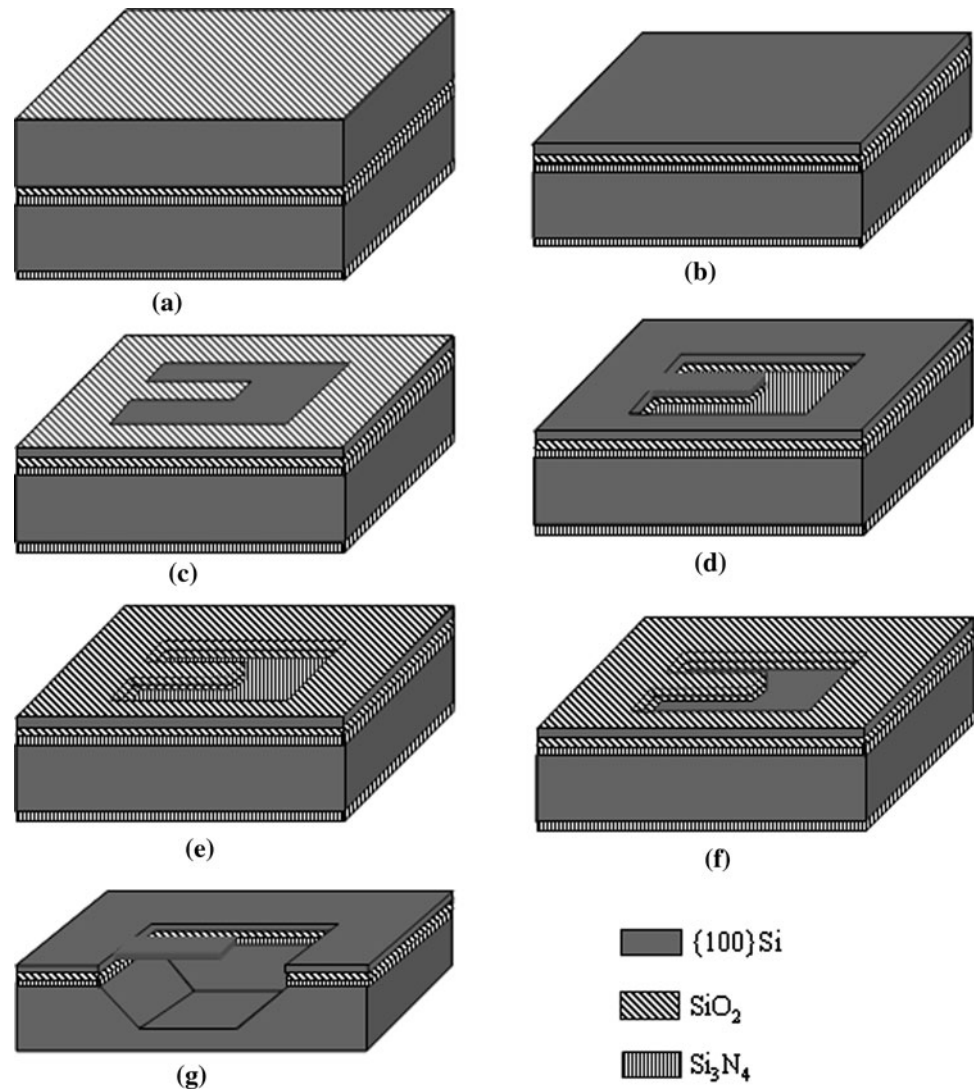


Fig. 3 Process steps for the fabrication of silicon cantilever beams using only single lithography step. **(a)** Direct wafer bonding between silicon nitride (Si_3N_4) and oxide (SiO_2) deposited wafers, **(b)** thinning down of the top wafer for structural layer up to desired thickness, **(c)** oxidation and patterning, **(d)** silicon etching in 25 wt.% TMAH + Triton in order to define the shapes of the structures followed by oxide etching, **(e)** Local oxidation of silicon (LOCOS), **(f)** Silicon nitride etching while protecting the backside, **(g)** Silicon anisotropic etching in 25 wt.% TMAH for releasing the structures followed by removal of nitride and oxide



In this paper, we report the etching results of pure and non-ionic surfactant ‘Triton-X-100 ($\text{C}_{14}\text{H}_{22}\text{O}(\text{C}_2\text{H}_4\text{O})_n$, $n = 9\text{--}10$)’ added TMAH with different concentrations. The optimized etching characteristics of pure and surfactant added TMAH are employed to develop the new fabrication methods to realize the conventional and unconventional shapes structures in single and bonded silicon wafers. The structures include both fixed and freestanding types. The novelty of the fabrication methods is to utilize only one photolithography step to realize both types of structures (i.e. fixed and suspended).

2 Experimental work

P-type Czochralski-grown of three inch diameter of {100} and {110} orientations silicon wafers are used to measure the etching characteristics such as the etch rates of {100}

Si and {110} Si, undercutting at rounded concave and sharp convex corners in pure and 0.1% (v/v) Triton-X-100 added TMAH solutions at different concentrations (10–25 wt.%). The {100} Si wafers are utilized to fabricate the different MEMS structures. Fabricated structures are divided in two categories: fixed and freestanding. Both types require only one photolithography step. The fabrication methods are summarized below:

2.1 Fixed structures

In this case, the structures are realized using single mask and one step wet etching. The process steps are schematically presented in Fig. 2. However the process is illustrated for square-shaped mesa structures, it is generic and same steps are used to fabricate other types of structures such as circular mesa and grooves, microfluidic channels, etc. Firstly, thermal oxidation is carried out to

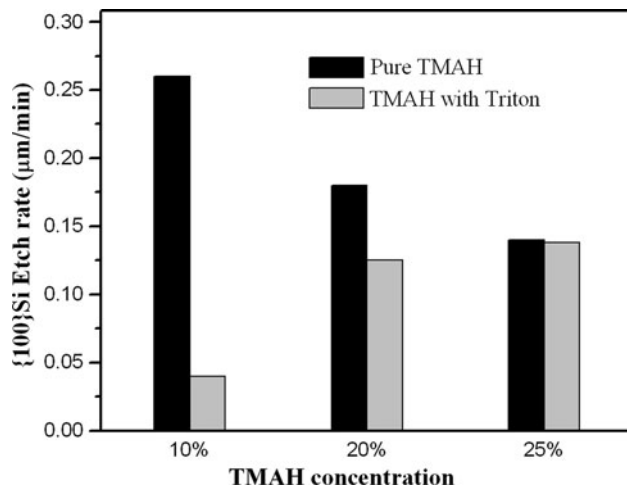


Fig. 4 Etch rates of {100} Si in different concentration of pure and Triton-X-100 added TMAH at 60°C

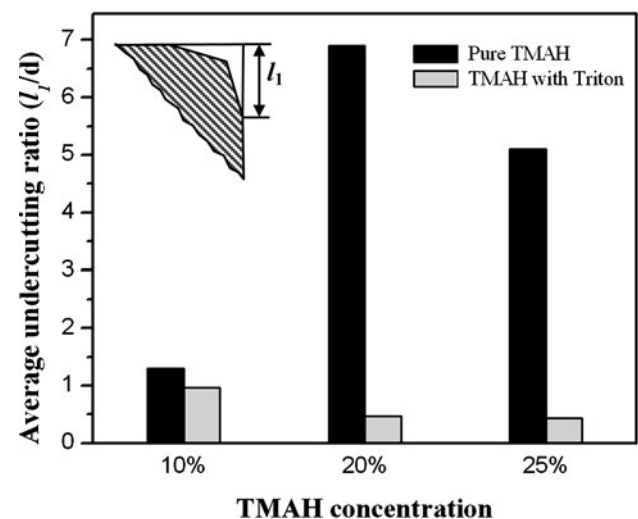


Fig. 6 Undercutting ratio at sharp convex corners (l_1/d) in different concentration of pure and Triton added TMAH at 60°C; l_1 : undercutting along $\langle 110 \rangle$ direction at convex corner, d etch depth at Si{100} wafer surface

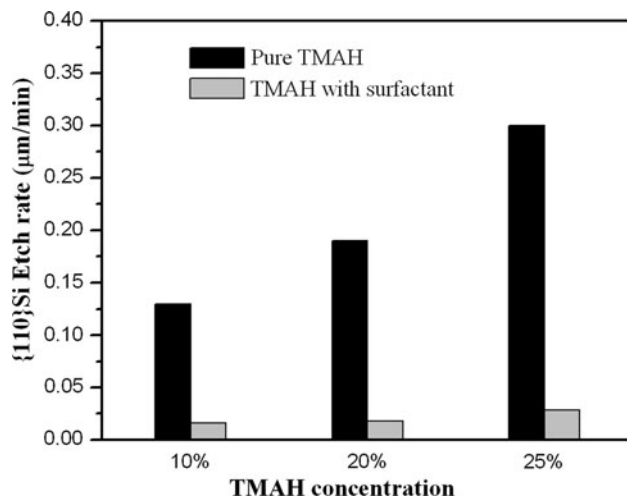


Fig. 5 Etch rates of {110} Si in different concentration of pure and Triton-X-100 added TMAH at 60°C

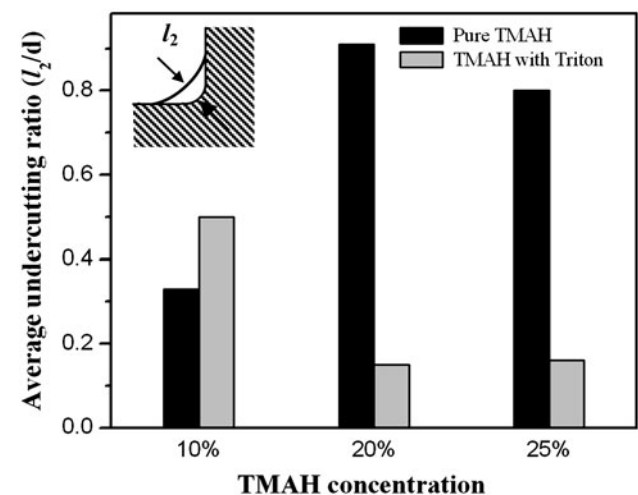


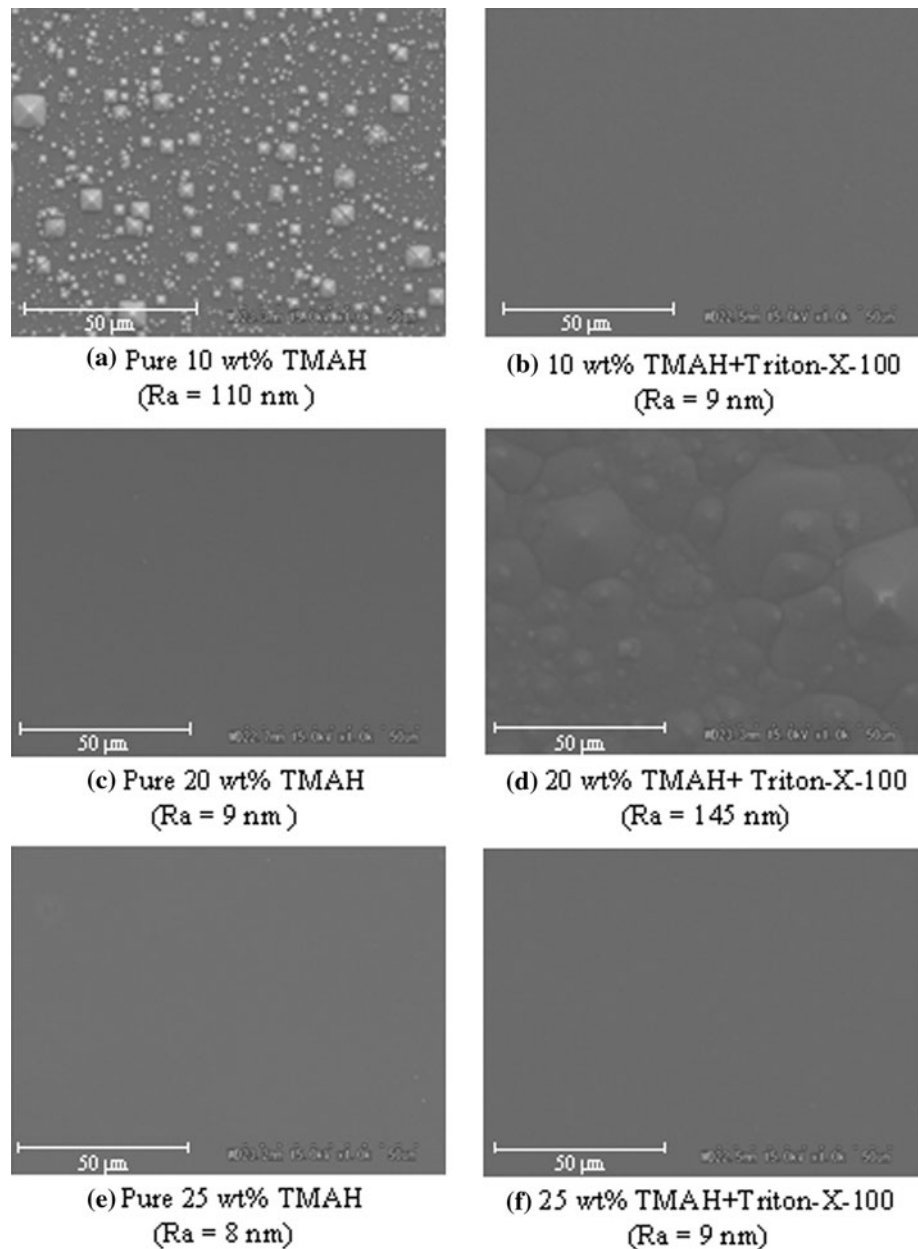
Fig. 7 Undercutting ratio at rounded concave corners (l_2/d) in different concentration of pure and Triton added 25 wt.% TMAH at 60°C; l_2 undercutting along $\langle 100 \rangle$ direction at rounded concave corner, d etch depth at Si{100} wafer surface

grow an oxide layer of about 0.5 μm thickness. The wafers are then patterned using photolithography followed by oxide etching in buffered hydrofluoric acid (BHF). Thereafter, wet anisotropic etching is performed in 25 wt.% TMAH + Triton (Fig. 2c). As discussed in the next section, the surfactant added TMAH provides minimum undercutting at all types of corners and edges. Prior to anisotropic etching, the wafers are cleaned properly in order to avoid the incorporation of any impurities in the etchant as the etching characteristics are very sensitive to them. After anisotropic etching, oxide layer is removed. The final shapes of square shaped mesa structures are schematically shown in Fig. 2d.

2.2 Suspended structures

In this method, the structures are released from the substrate by wet etching. Fabrication process utilizes wafer bonding, one lithography step, local oxidation of silicon (LOCOS) and two steps anisotropic wet etching. As described in the next section, pure TMAH, especially at high concentrations (20–25 wt.%), exhibits high undercutting at non-sharp concave and non- $\langle 110 \rangle$ etch mask edges on {100} Si surface, while surfactant added TMAH shows minimum undercutting at all types of corners and edges. Figure 3 shows the schematic representation of

Fig. 8 SEM photographs of {100} Si etched surface morphologies in different concentrations of TMAH without and with Triton X-100



process steps for the realization of suspended silicon structures. First, oxide and nitride deposited wafers are direct-bonded. Prior to bonding step, the wafer surfaces are activated using RCA cleaning solutions ($\text{HCl}:\text{H}_2\text{O}_2:\text{H}_2\text{O} = 1:1:5$ and $\text{NH}_4\text{OH}:\text{H}_2\text{O}_2:\text{H}_2\text{O} = 1:1:6$) (Ismail et al. 1990; Sanchez et al. 1997; Tong and Gosele 1999; Wiegand et al. 2000). The room temperature bonded wafers are annealed at $1,050^\circ\text{C}$ for 1 h in an oxygen environment to increase the bond strength. After this step, the thickness of oxidized wafer in bonded pair is reduced to a desire level by etching in pure (or surfactant added) 25 wt.% TMAH after removal of its oxide in BHF

(Fig. 3b). The chemical mechanical polishing (CMP) is employed to remove any hillocks on the etched surface. The bonded wafers are then oxidized thermally in order to grow the masking layer. Thereafter, the oxide layer is patterned by photolithography followed by oxide etching in BHF. After this step, anisotropic etching is carried out in 25 wt.% TMAH + Triton to define the shapes of the structures, followed by oxide etching (Fig. 3d). Now, LOCOS process is performed to grow an oxide layer on the exposed silicon. The nitride layer is then removed selectively in hot phosphoric acid (H_3PO_4). Finally, silicon etching is performed in pure 25 wt.% TMAH in order

Fig. 9 Schematic views of the etched profiles of square shaped mask opening when the etched depth is controlled by (a) {111} planes, (b) and (c) etch stop layers (e.g. SiO_2 , Si_3N_4 , $\text{P}^+\text{-Si}$, etc.). SEM picture shows an etched cavity in {100} Si bounded by {111} planes

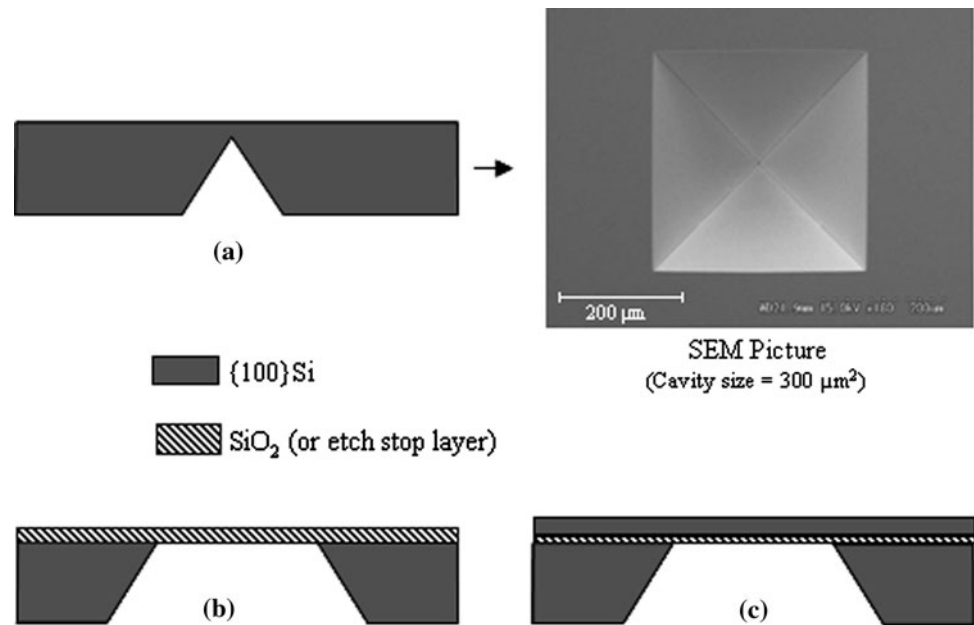
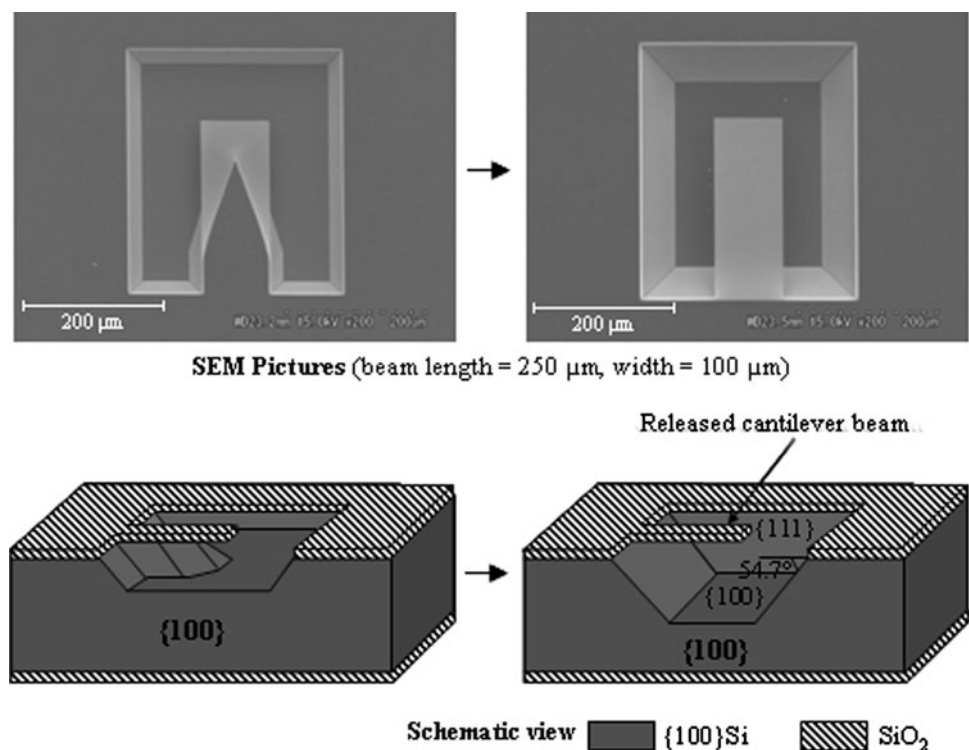


Fig. 10 Fabrication of SiO_2 (or Si_3N_4 or $\text{P}^+\text{-Si}$) cantilever beams on {100} Si wafers by wet anisotropic etchants. The fast undercutting at the convex corners facilitates the beam to release from the substrate



to release the structures from the substrate. This step is followed by nitride and oxide removal in H_3PO_4 and BHF, respectively. Of course, the schematics show the fabrication steps only for freestanding cantilever beams; in reality, the multiple structures with different shapes are

fabricated at once on a SOI wafer. It may be emphasized here that the bonding process is aimed to demonstrate the proposed fabrication technique. The detailed study of bonding process is beyond the scope and purpose of the present research.

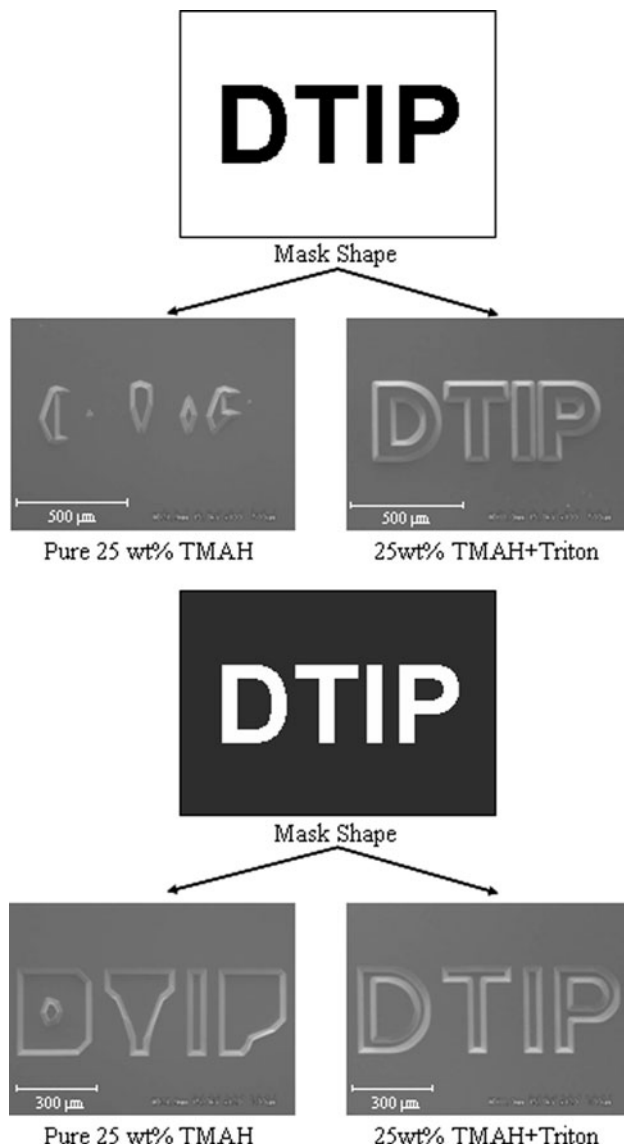


Fig. 11 Micromachining of alphabets in order to emphasize the effect of Triton in TMAH solution (Etch depth = 30 μm)

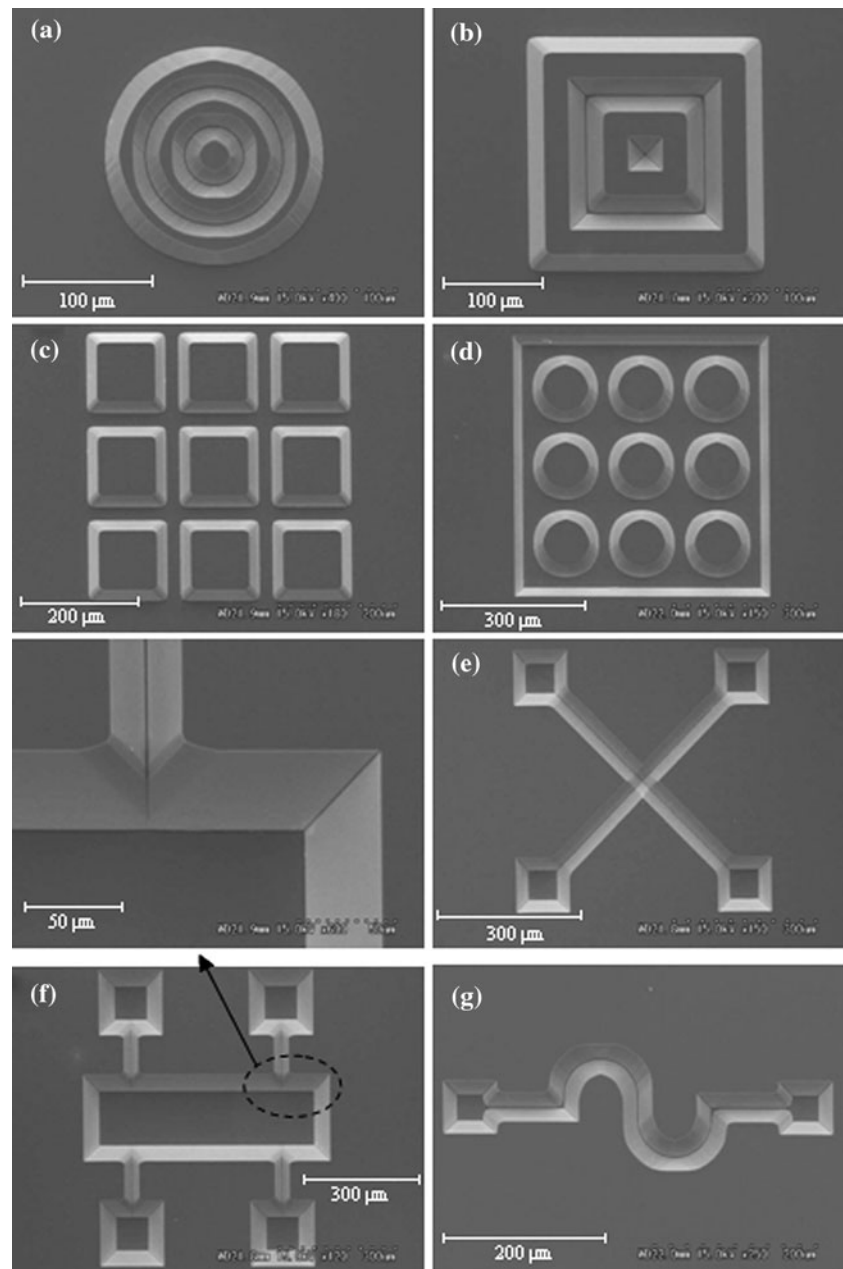
3 Results and discussion

The etch rates of $\{100\}$ and $\{110\}$ silicon, undercutting at sharp convex and rounded concave corners in different concentration of TMAH without and with addition of Triton-X-100 are presented in Figs. 4, 5, 6, 7, respectively. Etched surface morphologies are shown in Fig. 8. The mechanism behind the change in etching characteristics of pure TMAH when a small amount of surfactant is added into it is discussed elsewhere (Merlos et al. 1992; Pal et al. 2007b; Sundaram et al. 2005; Yang et al. 2005; Zubel and Kramkowska 2001). The $\{100\}$ Si substrate is the most widely used in silicon mainstream technology. The low concentration of pure TMAH (10 wt.% in this study)

provides highest $\{100\}$ Si etch rate (Fig. 4), but etched surface is full of hillocks (Fig. 8a). When surfactant is added in the solution, surface morphology improved dramatically (Fig. 8b, but etch rate suppressed significantly (Fig. 4). Hence, the low concentration of pure TMAH is a very useful choice when etched surface morphology is not a concern or to form the truncated shape cavities bounded by $\{111\}$ planes as shown in Fig. 9a. It can also be employed for the applications where etch stop layer is used to fabricate the structures, for instance, SiO_2 diaphragms (or other structures) in single wafer (Fig. 9b), and silicon diaphragms (or truncated cavities with square/rectangular bottom) in silicon on insulator (SOI) wafers through the backside etching (Fig. 9c). In the case of high concentration TMAH (25 wt.%), etch rate of $\{100\}$ Si is almost same in both types of etchant, while the etch rate of $\{110\}$ Si, undercutting at sharp convex and rounded concave corners are affected considerably when the surfactant is added into the solution. Conclusively it can be stated that the TMAH with high concentration provides two choices (i.e. low and high) for corner undercutting and $\{110\}$ Si etch rate. Hence, for the fabrication of suspended structures (e.g. cantilever beams) by undercutting, pure 25 wt.% (or 20wt.%) TMAH is the best choice. Figure 10 shows the sequential stages of SiO_2 cantilever beam during etch release step in pure 25 wt.% TMAH. On the other hand, 25 wt.% TMAH + Triton is the optimal choice when minimum undercutting at sharp convex and curved edges is desirable. In order to demonstrate the apparent difference in the etched profiles on $\{100\}$ Si in pure and surfactant added TMAH, bulk micromachining of a group of alphabets 'DTIP' in pure and Triton added 25 wt.% TMAH is performed. The SEM pictures of etched 'DTIP' are shown in Fig. 11. The letters micromachined in pure TMAH have lost their shapes and cannot be recognized, while those are etched in Triton added TMAH retain their original shapes. Figure 12 shows the SEM pictures of different shapes silicon structures fabricated in one step lithography and single anisotropic etching step using the fabrication steps illustrated in Fig. 2. From the fabricated structures it can obviously be concluded that any shape of the masking pattern can be etched conformally, of course, with slanted sidewalls due to crystallographic limitations of wet etching.

Figure 13 shows the SEM pictures of fabricated cantilevers beams of different thicknesses and microfluidic channels using the process steps presented in Fig. 3. The commonly used methods for the fabrication of silicon suspended structures using wet bulk micromachining require two lithography steps as shown in Fig. 1. The second lithography step requires accurate alignment with respect to the patterns on the other side of the wafer. As can be seen in the Fig. 1, the larger backside opening is required and that restrict the fabrication of densely arrayed

Fig. 12 SEM pictures of different shapes fixed structures fabricated in {100} Si wafer in one photolithography step. Fabrication steps are illustrated in Fig. 2



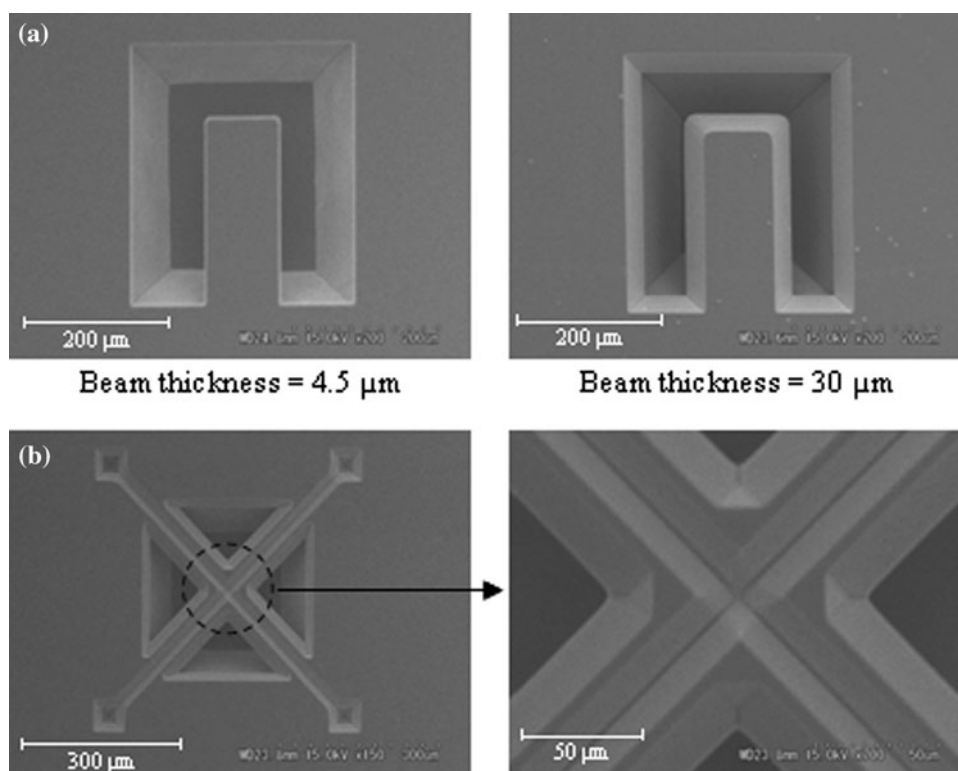
structures. As discussed in the previous section, the proposed fabrication technique requires only frontside process with one photolithography step. The method enables the fabrication of densely arrayed structures. Moreover, the time controlled etching during the releasing of the structures is not desirable.

4 Conclusions

The etching results such as {100} and {110} Si etch rates, corner undercutting, etched surface morphologies in

different concentrations of pure and Triton added TMAH are compared. Cross analysis of the etching results is presented in order to emphasize the applications of low and high concentration TMAH. The optimized etching characteristics are explored to develop the fabrication methods for the realization of fixed and freestanding structures. The fabrication method of fixed structures utilize only one photolithography and one etching step on single wafer, while freestanding structures require wafer bonding, photolithography, LOCOS and two steps wet etching. Both fabrication techniques provide the densely arrayed structures.

Fig. 13 SEM pictures of suspended silicon (a) cantilever beams (b) microfluidic channel in bonded wafers using the process steps described in Fig. 3



Acknowledgments This work was supported by Japan Society of the Promotion of Science (JSPS) through a foreign postdoctoral research fellowship scheme (2008–2010, fellowship ID No. 08053), and grant-in-aid for scientific research (A) 19201026, 70008053 from MEXT. We are grateful to Prof. Norikazu Suzuki for providing the chemical mechanical polishing (CMP) facility and for suggestions about how to use it successfully.

References

- Abedinov N, Grabiec P, Gotszalk T, Ivanov T, Voigt J, Rangelow IW (2001) Micromachined piezoresistive cantilever array with integrated resistive microheater for calorimetry and mass detection. *J Vac Sci Technol A* 19:2884–2888. doi:[10.1116/1.1412654](https://doi.org/10.1116/1.1412654)
- Bhardwaj J, Ashraf H, McQuarrie A (1997) Dry silicon etching for MEMS, proceedings of the 191st meeting Electrochemical Society. In: Proceeding of microstructures and microfabricated systems III symposium, Montreal, pp 118–130
- Conway EM, Cunnane VJ (2002) Electrochemical characterization of Si in tetra-methyl ammonium hydroxide (TMAH) and TMAH:Triton-X-100 solutions under white light effects. *J Micromech Microeng* 12:136–148. doi:[10.1088/0960-1317/12/2/307](https://doi.org/10.1088/0960-1317/12/2/307)
- Ismail MS, Bower RW, Veteran JL, Marsh OJ (1990) Silicon nitride direct bonding. *Electron Lett* 26:1045–1046. doi:[10.1049/el:19900677](https://doi.org/10.1049/el:19900677)
- Jeon JS, Raghavan S, Carrejo JP (1996) Effect of temperature on the interaction of silicon with nonionic surfactants in alkaline solutions. *J Electrochem Soc* 143:277–283
- Merlos A, Acero MC, Bao MH, Bausells J, Esteve J (1992) A study of the undercutting characteristics in the TMAH:IPA system. *J Micromech Microeng* 2:181–183. doi:[10.1088/0960-1317/2/3/014](https://doi.org/10.1088/0960-1317/2/3/014)
- Pal P, Sato K (2009a) Silicon microfluidic channels and microstructures in single photolithography step. In: Proceeding of symposium on design, test, integration and packaging of MEMS and MOEMS (DTIP-2009). Rome, Italy, pp 415–419
- Pal P, Sato K (2009b) Suspended Si microstructures over controlled depth micromachined cavities for MEMS based sensing devices. *Sens Lett* 7:11–16. doi:[10.1166/sl.2009.1003](https://doi.org/10.1166/sl.2009.1003)
- Pal P, Kim YJ, Chandra S (2006) Front-to-back alignment techniques in microelectronics/MEMS fabrication: a review. *Sens Lett* 4:1–10. doi:[10.1166/sl.2006.007](https://doi.org/10.1166/sl.2006.007)
- Pal P, Sato K, Chandra S (2007a) Fabrication techniques of convex corners in a (100)-silicon wafer using bulk micromachining: a review. *J Micromech Microeng* 17:R111–R133. doi:[10.1088/0960-1317/17/10/R01](https://doi.org/10.1088/0960-1317/17/10/R01)
- Pal P, Sato K, Gosalvez MA, Shikida M (2007b) Study of rounded concave and sharp edge convex corners undercutting in CMOS compatible anisotropic etchants. *J Micromech Microeng* 17:2299–2307. doi:[10.1088/0960-1317/17/11/017](https://doi.org/10.1088/0960-1317/17/11/017)
- Pal P, Sato K, Shikida M, Gosalvez MA (2009) Study of corner compensating structures and fabrication of various shapes of MEMS structures in pure and surfactant added TMAH. *Sens Actuators A* 154:192–203. doi:[10.1016/j.sna.2008.09.002](https://doi.org/10.1016/j.sna.2008.09.002)
- Resnik D, Vrtacnik D, Aljancic U, Mozek M, Amon S (2005) The role of Triton surfactant in anisotropic etching of 110 reflective planes on (100) silicon. *J Micromech Microeng* 15:1174–1183. doi:[10.1088/0960-1317/15/6/007](https://doi.org/10.1088/0960-1317/15/6/007)
- Sanchez S, Gui C, Elwenspoek M (1997) Spontaneous direct bonding of thick silicon nitride. *J Micromech Microeng* 7:111–113. doi:[10.1088/0960-1317/7/3/007](https://doi.org/10.1088/0960-1317/7/3/007)
- Sarro PM, Brida D, Vander Vlist W, Brida S (2000) Effect of surfactant on surface quality of silicon microstructures etched in saturated TMAHW solutions. *Sens Actuators A* 85:340–345. doi:[10.1016/S0924-4247\(00\)00317-4](https://doi.org/10.1016/S0924-4247(00)00317-4)

- Sekimura M (1999) Anisotropic etching of surfactant-added TMAH solution. In: Proceedings of the. 12th IEEE Micro-Electro-Mech System conference, Orlando, Florida, pp 17–21
- Sundaram KB, Vijayakumar A, Subramanian G (2005) Smooth etching of silicon using TMAH and isopropyl alcohol for MEMS applications. *Microelectron Eng* 77:230–241. doi:[10.1016/j.mee.2004.11.004](https://doi.org/10.1016/j.mee.2004.11.004)
- Tong QY, Gosele U (1999) *Semiconductor wafer bonding: science and technology*. Wiley, New York
- Wiegand M, Reiche M, Gosele U, Gutjahr K, Stolze D, Longwitz R, Hiller E (2000) Wafer bonding of silicon wafers covered with various surface layers. *Sens Actuators A* 86:91–95. doi:[10.1016/S0924-4247\(00\)00420-9](https://doi.org/10.1016/S0924-4247(00)00420-9)
- Wu Q, Lee M, Liu CC (1993) Development of chemical sensors using microfabrication and micromachining techniques. *Sens Actuators B* 13/14:1–6. doi:[10.1016/0925-4005\(93\)85310-7](https://doi.org/10.1016/0925-4005(93)85310-7)
- Yang CR, Yang CH, Chen PY (2005) Study on anisotropic silicon etching characteristics in various surfactant-added tetramethyl ammonium hydroxide water solutions. *J Micromech Microeng* 15:2028–2037. doi:[10.1088/0960-1317/15/11/006](https://doi.org/10.1088/0960-1317/15/11/006)
- Zubel I, Kramkowska M (2001) The effect of isopropyl alcohol on etching rate and roughness of (100) Si surface etched in KOH and TMAH solutions. *Sens Actuators A* 93:138–147. doi:[10.1016/S0924-4247\(01\)00648-3](https://doi.org/10.1016/S0924-4247(01)00648-3)